NAIC-ID(RS)T-0758-94

NATIONAL AIR INTELLIGENCE CENTER

ION ASSISTED DEPOSITION OF ZnS AND MgF_2 FILM

by

Gu Pei Fu, Chen Yuming, et al.

HUMAN TRANSLATION

NAIC-ID(RS)T-0758-94 1 May 1995

MICROFICHE NR: 95C000273

ION ASSISTED DEPOSITION OF ZnS AND MgF_2 FILM

By: Gu Pei Fu, Chen Yuming, et al.

English pages: 13

Source: Guangxue Xuebao, Vol. 9, Nr. 9, September 1989; pp. 815-822

Country of origin: China
Translated by: SCITRAN
F33657-84-D-0165
Requester: NAIC/TATD/Bruce Armstrong

GRAPHICS DISCLAIMER

All figures, graphics, tables, equations, etc. merged into this translation were extracted from the best quality copy available.

ION ASSISTED DEPOSITION OF ZnS AND MgF_2 FILM

/815*

Gu Pei Fu, Chen Yuming, Hu Xuequn and Tang Jinfa[1]

ABSTRACT

ZnS and MnF_2 films have been prepared by Ar ion assisted deposition.The packing density of MgF_2 has been increased from 0.8 to 0.9-0.95 without ion bombardment as determined by the wavelength shift measurement after moisture absorption by filter. It is shown that high energy bombardment (>1 keV) increases the absorption and scattering loss, while the low energy bombardment is shown to increase significantly the abrasion resistance and adherence of film without affecting the optical properties. Therefore, it will play a very important role in preparing durable coatings for temperature sensitive substrate.

Key Words: Ion assisted deposition, filter.

I. INTRODUCTION

Deposition of molecules on the surface of substrate or limited migration of atoms is one of the causes of film column structural growth. In 1980s, a proposal was made to increase the migratory ratio of depository ions and to improve the microstructure of the film by supplying certain amount of activation energy to evaporating molecules or atoms with ion bombardment technique. Studies (1-8) on oxide film ion assisted deposition revealed some interesting results. However, hardly any studies on ZnS and MgF_2 have been done except those by Herrmann and Kennemore et al. Hermann, et al obtained a MgF_2 film by bombarding the cold substrate with 50 $\mu A/cm^2$, 700 ev Ar ion which resulted in an

---

* Numbers in margins indicate foreign pagination. Commas in numbers indicate decimals.

[1] Dept. of Optical Engineering, Zhejiang Univ., Hang Zhou

increased adherence that is equivalent to the one obtained through depositing the hot substrate at 250°C. Kennemore, et al found that MgF_2 bombarded with low energy ion beams (<250 eV, 5-70 $\mu A/cm^2$) at room temperature had increased adherence and abrasion resistance, and had higher absorption in short waves (λ < 275nm). No through studies have been done on the optical stability of ZnS and MgF_2 film formed by ion assisted deposition. In order to further study the optical and mechanical properties of these films, we made ZnS and MgF_2 films by using ion assisted deposition. With high energy bombardment, the packing density of MgF_2 film can be reached as high as 0.95, but this is accompanied by higher absorption and abrasion. Bombarding with low energy ions, the adherence of film increases without losing desired optical properties. This practically paves the way for making durable film with room temperature substrate.

II. THE DESIGN OF THE EXPERIMENT

Three different kinds of ion source were used in the experiment. The first one is high energy (1-2 keV) ion emitting source made by Perkin-Elmer Inc. The ion is aimed at an angle of 30° from the vertical line of the substrate. The gun point is 13 cm from the vertical line of the substrate. The ion flowing density is 25-45 $\mu A/cm^2$. The working pressure is $8x10^{-5}$ Torr at room temperature.

The second one is a neutral particle source made by Ion Tech of Britain. It is powered by cold cathode direct current. High energy ions generated by equal ion entity recombine and form atoms under the influence of electro-static field near the output. In other words, it forms neutral particle beam. Such a particle source can avoid the damage on film crystal structure that is associated with electronic effect, it also can lower the bombardment efficiency caused by the electrons on the film surface. The

bombardment energy used in the experiment is 1.6-2.2 keV. The distance between the particle source and substrate varies from 6-10 cm for the purpose of adjusting the particle density of incoming particles. The particle beam has a 45° angle from the vertical line of substrate so as to ensure the even distribution of bombarding particles. The flowing density of the particles on the film is 10-20 $\mu A/cm^2$. Since a cathode is used, the working pressure can be as high as $5x10^{-4}$ Torr.

/816

The third kind is Kaufman type, in which the ion energy is 200-750 eV. The ion source is about 19 cm from the substrate. The ion flowing density on the substrate is 30-100 $\mu A/cm^2$. The substrate is lyophilized under $5-9x10^{-5}$ Torr.

Noteworthy, the first two are high energy bombardment, the third is low energy bombarding.

III. OPTICAL PROPERTIES

If we measure the wavelength shift after cooling the filter, we can solve the phase change $\alpha_{\phi H}$ and $\alpha_{\phi L}$, based on the heat expansion coefficient of ZnS(H) and MgF_2(L). Their relation with temperature can be expressed as (11)

$$\alpha_{\phi H}=(1.99\pm0.11)\times10^{-5}K^{-1},\ \alpha_{\phi L}=(0.91\pm0.06)\times10^{-5}K^{-1}.$$

In which K is absolute temperature. The peak value wavelength blue shift can be obtained given the temperature of substrates; vice versa.

On the other hand, the refractive index will change if the filter absorbs moisture from air. If ZnS has high packing density, we can focus on MgF_2 film. Change in refractive index or packing density is affected by many factors such as substrate temperature, evaporation rate and vacuum degree, etc. The primary

factor, substrate temperature is linked to the following equation (11):

$$\left(\frac{\delta N}{N}\right)_L = A_0 + A_1 \Delta\theta + A_2 (\Delta\theta)^2 (\%)$$

in which A_0=6.9, A_1=-4.46x10^{-2} and A2=9.35x10-5, $\Delta\theta$ is the change in substrate temperature. With this we can calculate expected $(\delta N/N)_L$ value and peak value wavelength red drift at different substrate temperature without bombarding, which can serve as contrast for the assisted case.

Three filters are used in the experiment. The first filter is bombarded at all layers; the second one is targeted at the inner surface and the layer which has low electronic field. The third filter is bombarded only at the low refractive index MgF_2 layer. The data is shown in table 1. Fig.1 shows the relationship among $(\delta N/N)_L$ and packing density P_L(=1-4.07 $(\delta N/N)_L$) and substrate temperature. Since deposition ratio (R) and vacuum degree (P) also affect these parameters, hence a characteristic factor Q is introduced. It defines a ratio of evaporating molecule to residual gas molecule.

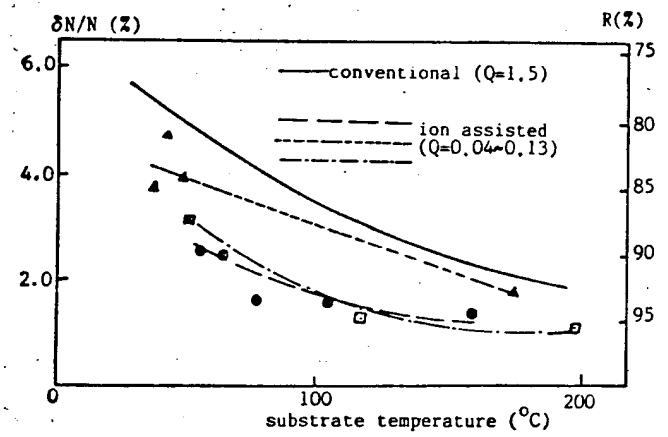

Fig. 1

Table 1 Experimental results of $ZnS-MgF_2$ filters with high energy ion-bombardment

type	design	bombarded parameter		filter properties				blue shift	sybstrate temp.	c vention			ion bombardment		
		keV	$\mu A/cm^2$	λ nm	T %	$\Delta\lambda$ nm	L^* %	nm	°C	$(\Delta N/N)_L$ $\times 10^2$	packing densiyt	red shift nm	$(\Delta N/N)_L$ $\times 10^2$	packing density	red shift nm
I	A|FLF|G F=HLH2LHLH	1.6	11	1226.0	90.4	64.	7.3	1.24	78.2	3.98	0.84	30.4	1.52	0.94	11.9
	A|M4LM|G M=(HL)^{3}H	2.2	14	657.9	73.3	8.	18.6	0.41	54.4	4.75	0.81	22.3	2.46	0.90	11.7
	A|M4LM|G M=(HL)^{3}H	1.6	13	641.9	71.2	5.	19.1	0.48	65.4	4.38	0.82	20.1	2.51	0.90	11.6
	A|2HM4LM|G M=(HL)^{3}H	2.2	14	658.3	62.3	7.5	20.0	0.80	105.3	3.24	0.87	15.4	1.53	0.94	7.4
	A|M4LM|G M=(HL)^{3}H	2.0	12	638.3	67.6	5.2	19.8	1.18	160.1	2.16	0.91	10.1	1.29	0.95	6.1
II	A|M4LM|G M=(HL)^{3}H	2.0	13	604.8	84.5	3.4	7.1	0.26	38.1	5.34	0.78	2.28	3.68	0.85	15.8
	A|M4LM|G M=(HL)^{3}H	2.0	13	610.0	80.0	3.5	6.8	0.30	44.0	5.12	0.79	21.9	4.86	0.80	20.8
	A|M4LM|G M=(HL)^{3}H	2.0	13	606.1	79.0	4.5	7.6	0.34	49.8	4.91	0.80	21.0	3.99	0.84	17.1
	A|M4LH|G M=(HL)^{3}H	2.0	13	597.1	76.4	4.8	8.0	1.20	175.7	1.95	0.92	8.5	1.93	0.92	8.4
III	A|FLF|G F=HLH4LHLH	1.8	13	1164.3	93	59	2.8	1.60	116.7	2.98	0.88	25.3	1.28	0.95	11.1
	A|FLF|G F=HLH4LHLH	1.9	13	1182.0	93	47	3.4	2.80	199.8	1.72	0.93	15.0	1.22	0.95	10.8
	A|M4LM|G M=(HL)^{3}H	1.8	14	558.0	76.4	3.3	18	0.32	51.0	4.87	0.80	19.3	3.25	0.87	12.9
	A|M4LM|G M=(HL)^{3}H	2.0	14	587.0	80.7	2.6	12.6	0.45	67.5	4.31	0.83	18.1	2.54	0.90	10.7

* The total lososes (absorption+seattering) at peak wavelength.

$$Q = 10^{-3} R/P$$

Apparently, $\delta N/N$ and P_L showed greater improvement despite the low values in fig.1.

If flowing density is increased, the wavelength drift can be reduced further. In film system A|M2LM|G,M=$(HL)^2H$ λ_0=530 nm, using 1 keV, 25 $\mu A/cm^2$ and 1.5 keV, 35 $\mu A/cm^2$ and 2.0 keV, 45 μA/cm2 ion beam for bombardment, the wavelength drift can be reduced to 2.6, 2.3 and 1.9 nm.

The filter discussed above is made by high energy ion assisted deposition. High energy ion bombardment invariably leads to higher losses. Usually, losses increase with the increase in ion energy, ion density and substrate temperature. Fig.2 is the measured absorption and scattering. Absorption of bombardment by 2 keV ions at λ = 633 nm is 1 numerical scale higher than the conventional method. This is caused by the change of chemical nature of the materials used.

Table 2 Measured losses for G|$(HL)^2H2LH(LH)^2$|A, λ_0=530 nm

loss		conventional		ion bombardment		
				1 keV, 25 $\mu A/cm^2$	1.5 keV, 25 $\mu A/cm^2$	2 keV, 45 $\mu A/cm^2$
absorption	1	0.011		0.026	0.049	0.142
	2	0.027		0.037	0.073	0.156
scatter	1	before coated	0.05	0.09	0.05	
		after coated	0.19	0.27	0.27	
	2	before coated	0.05	0.06	0.06	
		after coated	0.18	0.15	0.23	

Table 3 Experimental results of ZnS–MgF_2 filters with low energy ion bombardment

design	bombarded parameter (eV)	(μA/cm^2)	$\left(\frac{\Delta N}{\Lambda}\right)_L \times 10^2$	P_L	rod shift (nm)
Air|M2LM|G	conventional		7.13	0.71	29
M=(HL)^{2}H	500	104	3.90	0.84	16
λ_0=660 nm	750	110	3.65	0.85	15
	200	40	3.40	0.86	14
	300	60	3.40	0.86	14
Air|FLF$_1$|G	conventional		7.38	0.70	30
F=(HL)^2(LH)^2					
F$_1$=(HL)^3(LH)^3	700	110	3.65	0.85	15
λ_0=660 nm					
Air$\left\|A\frac{H}{2}B\frac{H}{2}A\right\|$G*	conventional		6.47	0.73	32
$A=\left(\frac{H}{2}L\frac{H}{2}\right)^2$					
$B=\left(\frac{L}{2}H\frac{L}{2}\right)^5$	200	40	3.98	0.84	20
λ_0=960 nm					

* A polarizer with detuned spacers operates at 1.06 μm. The results in table 3 refer to values of wavelength of 820 nm at normal incidence.

/819

The results of low energy bombardment are shown in table 3 and 4. Although, the optical adherence that is associated with low energy bombardment is not comparable to that of high energy bombardment, the losses can be reduced greatly.

Table 4 Measured losses of filters with low energy bombardment at λ=633 nm

design	absorption		scatter		bombarded parameter	
	conventional	ion-assisted	conventional	ion-assisted	eV	μA/cm^2
Air|H2LF|G F=(HL)^2(LH)^2	3.6×10^{-3}	4.2×10^{-3}	4×10^{-3}	7.4×10^{-4}	300	60
5-layer filter	4.6×10^{-4}	4.9×10^{-4}			400	65
Air$\left\|A\frac{H}{2}B\frac{H}{2}A\right\|$G $A=\left(\frac{H}{2}L\frac{H}{2}\right)^2$ $B=\left(\frac{L}{2}H\frac{L}{2}\right)^5$	1.2×10^{-3}	8.6×10^{-3}	1×10^{-2}	6.7×10^{-3}	200	40

We should point out that ZnS-MgF_2 multilayer film carries certain wavelength drift even after ion bombardment, and drift rate is three times faster than the filter made with conventional methods. This shows that ion bombardment can lead to shrinkage in space among column crystals.

IV. MECHANICAL PROPERTIES

In order to test the stress of the film formed by ion assisted bombarding, a stress testing device (19) similar to the one described by Heavens (19) was made. A steel ball with 0.125 mm radius was used to roll on the film to induce scratch, and scratch depth and width were determined by Talystep. Table 5 list data on high energy bombardment on ZnS and MgF_2 single layer films. According to Hertzian theory, glass substrate deforms and has a load under the steel ball, the contact radius of the steel ball is

$$a=\sqrt{\frac{Wg}{P\pi}} \text{ (cm)},$$

When, W=load (g), g=980 cms^{-2}, P is the hardness of the glass scratch (=$4x10^{10}$ dan • cm^2). The experimentally determined scratch width after bombarding the film in
Table 5 is very close to the calculated value using this formula (68 μm). This demonstrated that the load is very close to the value of the deformed glass. In other words, the film bombarded by high energy ions is as hard as glass, and it has excellent adhesion.

Table 5 Scratch depths and widths determining by Talystep

layer	bombardment	load(g)	scratch depth (nm)	scratch width (μm)
ZnS	no	25	42±7	4±2
	yes	1500	1.5±0.6	85±5
MgF_2	no	10	12±5	4.6±2
	yes	1500	2±1.2	80±6

The stress of the film after low energy bombardment is lower than that of high energy bombardment. It has sizable improvement over the conventional method. Table 6 shows some of the experiment results.

The improvement in film stress is contingent upon its adhesion and hardness. However, the interacting force within MgF_2 can also play an important role. Table 7 compiled measured parameters on ZnS, MgF_2 and Na_3AlF_6 using cat-eye interometer.Table 7 can shed more light on the reason why ion assisted ZnS-Na_3AlF_6 filter is more fragile than the one obtained thru conventional methods.

Table 6 Test results of the mechanical properties of films

coating	bombarded parameter		scratch test			scratch with pencil		tape test		30% HCl(min)	
	eV	μA/cm²	dloa (g)	turns conntional	turns bombardment	conventional	bombardment	conventional	bombardment	conventional	bombardment
Zn	200	60	30	1	>30	nondamage	nondamage	nondamage	nondamage	5	13
$8MgF_2$	200	60	20	1	>30					25	120
9-layer filter	300	60	10	2	16	4B	HB	1次坏	nondamage	damage in water	120
5-layer filter	400	65	10	1	11	2B	4H	nondamage		—	—
21-layer polarizor	200	40	10	1	12	4B	2H	damage after one	damage after 3 time	damage in water	1

Table 7 Stress of films with high energy ion bombardment

film	stress(kgf/cm²) conventional	stress(kgf/cm²) bambardment
ZnS	710±200	1133±200
MgF_2	2502±200	1250±200
Na_3AlF_6	326±200	611±200

V. STRUCTURAL PROPERTIES AND ANTILASER DAMAGE CRITICAL VALUES

Examination on ZnS-MgF_2 single layer film and multilayer film by electron microscope has shown, ZnS film bombarded by high energy, high density ions tends to be nonstructural, while MgF_2 film tends to form columns. Analysis on the composition of ZnS and MgF_2 has shown that bombarded MgF_2 film is de-fluorinized. This ZnS film also has different composition in comparison to the conventional one.

Table 8 The results of laser damage

coating	later damage (J/cm^2)		bombarded parameter and later
	conventional	bombarded	
$ZnS\left(\frac{\lambda_0}{4}\right)$	12.5	14.5	1keV 25$\mu A/cm^2$ HWFM 18ns
$MgF\left(\frac{\lambda_0}{4}\right)$	15.4	24.8	
11-layer filter	5.4	4.0	
13-layer mirror	4.0	3.6	
$ZnS\left(\frac{\lambda_0}{4}\right)$	9.1	11.2	300eV 45$\mu A/cm^2$ HWFM 10ns
$MgF_2\left(\frac{\lambda_0}{4}\right)$	9.0	12.7	
9-layer filter	1.8	1.8	
21-layer polarizor	0.7	1.2	

Due to the change in optical property, mechanical property and structure, the laser damage critical values of the assisted film go up except for the middle layer film bombarded by high energy. Table 8 shows the result of laser damage, laser wavelength is 1.06 μM.

VI. CONCLUSIONS

Ion assisted deposition is not as effective as most oxides in promoting the optical stability of ZnS-MgF_2 film regardless of the magnitude of bombardment. High energy bombardment is more effective in reducing wavelength drift and in improving packing density than low energy bombardment. But it can also lead to higher optical loss, therefore we can not expect it will improve the overall optical properties of the films. Since it can improve the stability of films, especially the possibility to make durable optical film with heat sensitive substrate, this makes it possible for expanded application of these materials. With this technology, we made ZnS-MgF_2 multilayer films on Fabry-Perot set-up and at the end of optical fiber.

Acknowledgement: We thank Dr Lissberger of British Royal University for his assistance in this study. We also want to thank Lu Zhong Liang for the measurements on absorption and scattering.

REFERENCES

[1] P. J. Martin, H. A. Madeod *et al.*; *Appl. Opt.*, 1983, **22**, No. 1 (Jan), 178.
[2] John R. Mcneil, Alan, C. Barron *et al.*; *Appl. Opt.*, 1984, **23**, No. 4 (Fab), 552.
[3] Wayne G. Sainty, R. P. Netterfield *et al.*; *Appl. Opt.*, 1984, No. 7 (Apr), 1116.
[4] Steven G. Saxe, M. J. Messerly *et al.*; *Appl. Opt.*, 1984, **23**, No. 20 (Oct), 3633.
[5] John R. Mcneil, G. A. Al-Jumaily *et al.*; *Appl. Opt.*, 1985, **24**, No. 4 (Feb), 486.
[6] H. Demiryont, James R. Sites *et al.*; *Appl. Opt.*, 1985, **24**, No. 4 (Feb), 490.
[7] Roger P. Nettefield, W. G. Sainty *et al.*; *Appl. Opt.*, 1985, **24**, No. 14 (Jul), 2267.
[8] P. J. Martin; *J. Mater. Sci.*, 1986, **21**, 1.
[9] W. C. Herrmann, J, R, Mcneil; *Proc. SPIE*, 1982, **325**, 101.
[10] Charles M. Kennemore, Ursula J. Gibson; *Appl. Opt.*, 1984, **23**, No. 20 (Oct), 3608.
[11] P. H. Lissberger *et al.*; *Optical Acta*, 1986, **33**, No. 7, 925.
[12] O. S. Heavens; *J. Physics and Radiation*, 1950, **11**, 355.
[13] 陈宇明,唐晋发等;《光学学报》, 1986, **6**, No. 1 (Jan), 70。

DISTRIBUTION LIST

DISTRIBUTION DIRECT TO RECIPIENT

ORGANIZATION	MICROFICHE
B085 DIA/RTS-2FI	1
C509 BALLOC509 BALLISTIC RES LAB	1
C510 R&T LABS/AVEADCOM	1
C513 ARRADCOM	1
C535 AVRADCOM/TSARCOM	1
C539 TRASANA	1
Q592 FSTC	4
Q619 MSIC REDSTONE	1
Q008 NTIC	1
Q043 AFMIC-IS	1
E051 HQ USAF/INET	1
E404 AEDC/DOF	1
E408 AFWL	1
E410 AFDTC/IN	1
E429 SD/IND	1
P005 DOE/ISA/DDI	1
P050 CIA/OCR/ADD/SD	2
1051 AFIT/LDE	1
P090 NSA/CDB	1
2206 FSL	1

Microfiche Nbr: FTD95C000273
NAIC-ID(RS)T-0758-94